JAYPEE INSTITUTE OF INFORMATION TECHNOLOGY, NOIDA

MINOR PROJECT ODD SEMESTER 2024

<u>MINOR PROJECT – 1</u>

<u>TOPIC:</u> Modelling of Substrate Integrated Waveguide and Comparison with WR90 in ANSYS HFSS

Submitted By:

Parth Sai Dhar (22102036)
Aarush Gupta (22102062)

Under the Supervision of:

Dr. Reema Budhiraja

Department of ECE

Jaypee Institute of Information Technology, Noida, U.P., India
<u>TABLE OF CONTENTS</u>

CERTIFICATE

This is to certify that the work which is being presented in B.Tech Minor Project Report entitled: "Modelling of Substrate Integrated Waveguide and Comparison with WR90 in ANSYS HFSS", submitted by: Parth Sai Dhar (22102036) & Aarush Gupta (22102062) , in partial fulfilment of the requirements for the award of degree of Bachelor of Technology in Electronics & Communication Engineering and submitted to the Department of Electronics & Communication Engineering of Jaypee Institute of Information Technology, Noida is an authentic record of our own work carried out during a period from August 2024 to November 2024 under the supervision of "Dr. Reema Budhiraja", ECE Department. The matter presented in this report has not been submitted by us for the award of any other degree elsewhere.

This is to certify that the above statement made by the candidates is correct to the best of my knowledge.

Dr. Reema Budhiraja (Supervisor)

<u>ACKNOWLEDGEMENT</u>

The success and final outcome of this project would not have been possible without the able guidance, we are extremely fortunate to have got this throughout the completion of the project work. We hereby take this opportunity to thank and show our gratitude towards everyone who supported us.

We thank our professor, project guide Dr. Reema Budhiraja for guiding us throughout the way and for advising us on various aspects of our project. We thank her for offering much appreciated and sought-after advice and suggesting thought-provoking ideas throughout the semester. We are indebted to our guide for offering us the freedom to explore and work on challenging aspects of the project. Her constant support and guidance have helped us complete our project successfully.

With sincere thanks

CHAPTER 1: INTRODUCTION

A waveguide is a structure that guides waves by restricting the transmission of energy to one direction. Common types of waveguides include acoustic waveguides which direct sound, optical waveguides which direct light, and radio-frequency waveguides which direct electromagnetic waves other than light like radio waves.

The concept of waveguides extends beyond the electromagnetic domain to encompass various types of waves, including radio frequency (RF), optical, acoustic, and even mathematical waveguides. While they differ in terms of the physical nature of the waves they guide and the mediums involved, the underlying principles are quite similar.

Key Differences:

-Radio Frequency Waveguides: Closely related to traditional electromagnetic waveguides like rectangular or SIWs, but vary based on frequency range.

-Optical Waveguides: Handle much higher frequency electromagnetic waves (light) and require dielectric materials for guiding. They are similar to RF waveguides in their use of boundary conditions but operate at a much higher frequency.

-Acoustic Waveguides: Guide mechanical waves like sound, not electromagnetic waves. The wave propagation in acoustic waveguides follows similar principles (modes, boundary reflection) but with significantly lower frequencies.

- Mathematical/Quantum Waveguides: These are more abstract but still follow waveguide theory principles. They extend the waveguide concept to quantum and theoretical realms, often dealing with particles or theoretical wave phenomena.

In this project, we will focus mainly on rectangular waveguides (and its variants i.e. SIW), which are a hollow metallic tube with a rectangular cross section. When the waves travel longitudinally down the guide because of conducting walls plane waves are reflected from wall to wall. This process results in a component of either electric or magnetic field in the direction of propagation of the resultant wave. Any uniform plane wave in a lossless guide may be resolved into TE and TM waves. In rectangular guide the modes are designed TE_{mn} or TM_{mn}.

Substrate-integrated waveguide (SIW) is a modern day (21st century) transmission line that has recently been developed. This technology has introduced new possibilities to the design of efficient circuits and components operating in the radio frequency (RF) and microwave frequency spectrum. Microstrip components are very good for low frequency applications but are ineffective at extreme frequencies, and involve rigorous fabrication concessions in the implementation of RF, microwave, and millimetre-wave components. This is due to wavelengths being short at higher frequencies. Waveguide devices, on the other hand, are ideal

for higher frequency systems, but are very costly, hard to fabricate, and challenging to integrate with planar components. SIW connects the gap that existed between conventional air-filled rectangular waveguide and planar transmission line technologies including the microstrip.
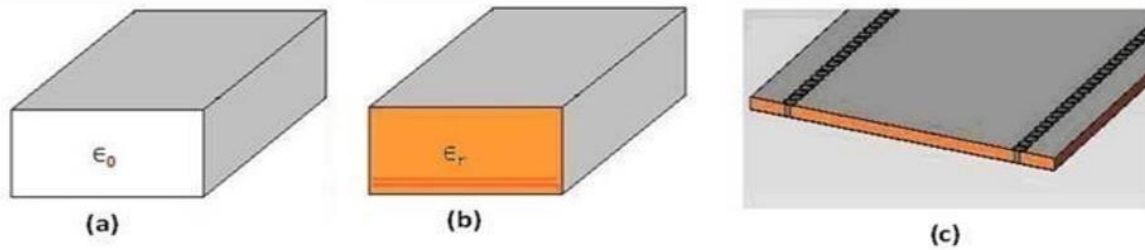

Fig1.1: a) Air-filled rectangular waveguide b) Dielectric-filled rectangular waveguide c) Substrate integrated waveguide

Electromagnetic waves of frequencies varying from 300 MHz up to 300 GHz stay classified as microwaves. This frequency span matches the free space wavelengths of 1m to1mm, in that order. Electromagnetic waves of frequencies varying from 30 GHz to 300 GHz stay classified as millimetre-waves due to having wavelengths that lay directly over 1 mmanddirectlyunder10mm. The RF band falls somewhere beneath the microwave range, though the border in the middle of the radio frequency and microwave bands is subjective and changes based on the method established for developing the band.

1.1   Structure of Waveguide

Rectangular waveguides are basically rectangular metallic cross section which may be hollow or filled with dielectric material. When the waves travel longitudinally down the guide because of conducting walls plane waves are reflected from wall to wall. This process results in a component of either electric or magnetic field in the direction of propagation of the resultant wave. Any uniform plane wave in a lossless guide may be resolved into TE and TM waves. In rectangular guide the modes are designed TE_{mn} or TM_{mn}.

SIW transmission line is basically a dielectric-filled waveguide implemented by two lines of conducting posts (also known as vias) implanted within a dielectric substrate, and electrically connecting the top and the bottom conducting walls. The substrate-integrated waveguide retains the benefits of a microstrip, including compactness and ease of integration, while also retaining some of the waveguide attributes, including minimal radiation loss, elevated unloaded Q-factor, and the elevated power processing capacity. The important advantage of the SIW transmission line technology is the opportunity to combine various devices (both active and passive) on a single substrate.

CHAPTER 2: DESIGN BASICS

2.1 Modes of Propagation

Rectangular waveguides support two types of wave modes:

- TE (Transverse Electric) Modes: The electric field is purely transverse (i.e., no electric field component along the direction of propagation).

- TM (Transverse Magnetic) Modes: The magnetic field is purely transverse (i.e., no magnetic field component along the propagation direction).

The dominant mode in rectangular waveguides is the TE_{10} mode, which has the lowest cutoff frequency and is the most commonly used mode.

Substrate-integrated waveguides and the traditional air-filled waveguide have comparable characteristics, as both technologies provide for $TE_{i,0}$ modes including TE_{10}, the dominant mode. Nevertheless, as opposed to the traditional air-filled waveguide which can maintain TM and $TE_{i,j}$ ($j \neq 0$) modes, the substrate-integrated waveguide is not able to maintain these modes due to the discontinuity in the side walls. Consequently, only the $TE_{i,0}$ modes can be supported in the SIW structure. The external current circulation of a conventional waveguide, with metallic posts on the thin walls, can be used to describe the fact of the presence of $TE_{1,0}$ mode in the substrate-integrated wave guide, as shown in figure. This is due to surface currents being formed in guided wave constructions because of mode formation. Significant energy radiation should happen when the holes cut all the length of the current's transverse path. Alternatively, only an extremely small amount of radiation should happen when the holes cut through the path of current flow. It can be observed that the holes do not cut the surface current on the side metallic wall. Hence, the $TE_{1,0}$ mode is maintained in the structure, which clarifies why the $TE_{i,0}$ modes can happen in the substrate-integrated waveguide structure.
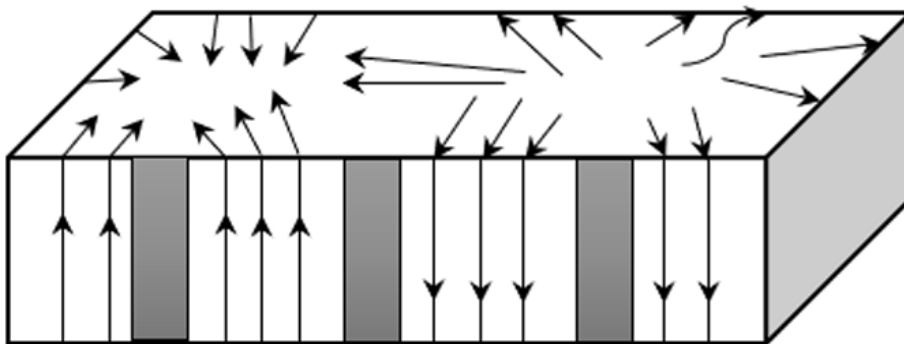

Fig 2.1.1: Surface current distribution of waveguide with metallic holes on thin side walls

2.2 Fundamental Design Parameters

Three fundamental design parameters must be considered when designing the substrate-integrated waveguide to function at an assigned frequency. These parameters include the substrate-integrated waveguide width, w, the metal via diameter, d, and the space or separation length between adjacent metal vias (that is, the pitch), p.

Similar to the width of the conventional rectangular waveguide, the substrate integrated waveguide width relates to the cut-off frequency of its propagation mode. The d and the p parameters define the close relationship between the substrate-integrated waveguide structure and the rectangular waveguide. Reducing the value of p to to d/2 essentially reduces the SIW to a regular dielectric-filled waveguide. Increasing the value of p increases the amount of the SIW deviation from the conventional rectangular wave guide, with more EM energies emitting outward in the middle of the vias. Substrate-integrated waveguide fundamental design parameters.

The design parameter Weff gives the substrate-integrated waveguide effective width, leff gives its effective length, μr is the substrate relative permeability (μr = 1 if substrate material is non-magnetic), εr is the substrate material dielectric constant, while c gives the free space speed-of-light. Experimental formulations for the weff and the leff are provided in equations given below.
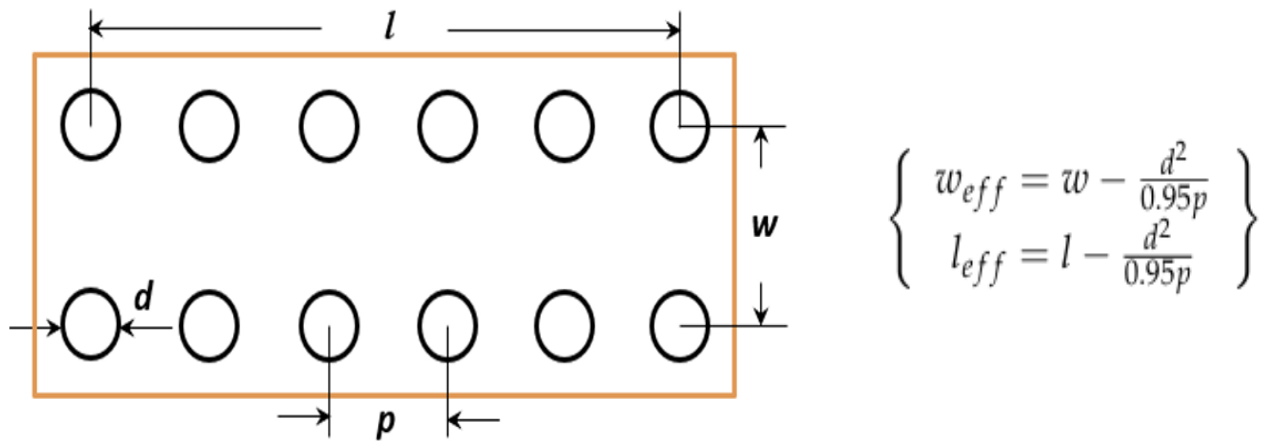

$$\left\{ \begin{array}{l} w_{eff} = w - \dfrac{d^2}{0.95p} \\[2mm] l_{eff} = l - \dfrac{d^2}{0.95p} \end{array} \right\}$$

Fig 2.2.1: Top view of SIW with design parameters

CHAPTER 3: DESIGN EQUATIONS

3.1 Cut-Off Frequency

Dimensions of waveguides operating in different frequency bands from C band to K band with cut-off frequency fc are calculated. Design rules mentioned in the above section are followed for SIW to avoid band-gaps and leakage/radiation loss in operating frequency band. Pitch p is kept twice the via diameter d. Dimensions of SIW are calculated using Weff above.

$$f_c = \frac{c}{2W_{\text{eff}}\sqrt{\varepsilon_r}} \qquad\text{(3.1)}$$

Here, fc is the cutoff frequency of SIW in the TE10 mode. For the rectangular waveguide, we have considered it to be air filled for simplification and its cut off frequency is given as below:

$$f_c = \frac{c}{2}\sqrt{\left(\frac{m}{a}\right)^2 + \left(\frac{n}{b}\right)^2} \qquad\text{(3.2)}$$

Where, c is the speed of propagation of light in air, 'a' is considered to be the broader dimension (which is the physical width of the waveguide), 'b' is considered to be the narrow dimension which is the physical height of the waveguide. Whereas 'm' and 'n' are the number of half cycles along a and b respectively.

For the sake of comparison, we will be comparing the performance of both waveguides in TE10 mode which further simplifies the fc of rectangular waveguide to:

$$f_c = \frac{c}{2a} \qquad\text{(3.3)}$$

3.2 Losses

Waveguides have two types of losses: dielectric loss and conductor loss, which can be calculated using equations given below and are taken from [7] :-

$$\alpha_d = ((k^2\tan\delta))/2\beta \qquad\text{(3.4)}$$

$$\alpha_c = R_s \frac{(2h\pi^2 + S^3k^2)}{S^3 h\beta k\eta} \qquad\text{(3.5)}$$

$$\beta = \sqrt{k^2 - k_c^2}$$

-- (3.6)

$$k = 2\pi f \sqrt{\mu\varepsilon}$$

-- (3.7)

$$k_c = 2\pi f_c \sqrt{\mu\varepsilon}$$

-- (3.8)

-- (3.9)

$$\eta = \sqrt{\mu/\varepsilon}$$

$$R_s = \sqrt{\omega\mu_0/2\sigma}$$

-- (3.10)

Where,

S and h are width and height of waveguide, respectively.

k is free space wave number.

β is phase constant.

$\tan\delta = 0.0012$ is the dielectric loss tangent.

μ and ε are absolute permeability and permittivity, respectively.

η is wave impedance in the dielectric.

$\sigma = 5 \times 10^7$ S/m is conductivity of metal.

R_s is surface resistivity of the conductors.

f_c is cut-off frequency, and f is operating frequency.

Total loss α_t, in a waveguide, is therefore given by

$$\alpha_t = \alpha_d + \alpha_c$$

For SIWs , other than the two types of losses found in your standard waveguides, there is one additional loss- Leakage loss. It is of critical importance to know from which point the leakage losses in the SIW become prohibitive. We can use the conventional rectangular waveguide equation to calculate the dielectric and conductor losses in an SIW. Analytical equations for the dielectric and conductor losses in a rectangular waveguide, can be rewritten as

$$\alpha_d = \frac{k_0^2 \tan \delta}{2k_z} \quad \text{------------------------------- (3.11)}$$

$$\alpha_c = \frac{R_m}{a_e \eta \sqrt{1 - \frac{k_s^2}{k_0^2}}} \left[\frac{a_e}{b} + 2\frac{k_c^2}{k_0^2} \right] \quad \text{----------------------- (3.12)}$$

$$k_z(f) = \sqrt{k_0^2 - \left\{ \frac{2}{a_e} \cot^{-1}\left[\frac{f_c}{f} r_S(1 - j) \right] \right\}^2} \quad \text{------------------- (3.13)}$$

$$\alpha_r = \frac{\frac{1}{w}\left(\frac{d}{w}\right)^{2.84}\left(\frac{s}{d} - 1\right)^{6.28}}{4.85\sqrt{\left(\frac{2w}{\lambda}\right)^2 - 1}} \quad \text{------------------------------------- (3.14)}$$

Where Kz is a complex propagation constant, 'ae' is affective value of width ('a' or 'w'), rs is real part of the surface wave impedance, and λ is wavelength in dielectric.

SIW radiation loss, as opposed to conductor loss and dielectric loss, is overtly connected to the substrate-integrated waveguide itself. This is because of the periodic gaps occurring in the middle of the metal vias, which are implanted in the dielectric substrate. The radiation loss in substrate-integrated waveguide components is due to energy outflow out of these gaps. The radiation loss in substrate-integrated waveguides maybe overlooked when the metalized hole diameter d and the pitch p are selected in accordance with below equations, where λg is the guided wavelength in the substrate-integrated waveguide. The condition should guarantee that radiation loss is maintained at the lowest possible level that renders it insignificant. This implies that the substrate-integrated waveguide can be developed as a traditional dielectric-filled rectangular waveguide.

$$d < \lambda_g/5 \quad and \quad p \le 2d \quad \text{------------------------------------- (3.15)}$$

3.3 Substrate Selection

Before modelling the waveguides, it is imperative to decide what substrate we are going to keep between the metallic planes. The relative permittivity εr of the substrate plays a critical

role in determining the cutoff frequency. A higher dielectric constant leads to a lower cutoff frequency because the speed of wave propagation is reduced inside the substrate. Since we are keeping the rectangular waveguide air filled for the sake of this project, we just need to choose it for SIW. The physical size of SIW is directly linked to relative permeability or dielectric constant of material used. Higher value of dielectric constant also mean decrease in size of SIW. Insertion loss is also dependent on dielectric loss , other than substrate thickness and copper foil. Thermal expansion and thermal coefficient of permittivity of substrate material determines the temperature stability of SIW device. Peak power handling capability is also linked to substrate dielectric strength. Keeping all of this in mind , substrate selection becomes an integral part of the process of modelling a waveguide.

Inserting a dielectric substrate in waveguides, especially in Substrate Integrated Waveguides (SIWs), is a trade-off decision that balances the benefits of compact, low-cost, and integrated waveguide structures with the drawbacks of potential dielectric losses. Using a dielectric substrate reduces the wavelength of the signal within the waveguide, allowing for smaller waveguide dimensions compared to traditional air-filled waveguides. This is essential in applications where space is limited.

A dielectric substrate allows waveguides to be fabricated on printed circuit boards (PCBs) or similar planar platforms, which is critical for integration with other circuit components such as microstrip lines, coplanar waveguides, antennas, and active electronic components. For applications in microwave and millimetre-wave frequencies, SIWs allow designers to integrate multiple components on a single substrate, creating a compact system-on-substrate design.

SIWs can be manufactured using standard PCB fabrication techniques, which are cost-effective and scalable for mass production. This reduces the need for expensive precision machining required for traditional hollow metal waveguides. Unlike traditional waveguides, which may require complex alignment and assembly, SIWs are simpler to produce and align due to their planar structure and compatibility with PCB technology.

Dielectric substrates allow easy integration with active components (like amplifiers and mixers) and passive components (like filters, couplers, and antennas) on the same substrate. This enables the creation of compact, multifunctional circuits, which are essential in modern communications and radar systems.

For systems that involve both RF/microwave and digital or control circuitry, having a single substrate provides a seamless integration platform, allowing for compact and lightweight devices.

Dielectric-based waveguides, like SIWs, are particularly useful at microwave and millimetre-wave frequencies , where the reduced size, cost, and integration benefits of dielectric substrates outweigh the slight increase in loss.

Many dielectric substrates are engineered for low loss at high frequencies, minimizing the impact of dielectric losses and making them suitable for wideband applications.

While dielectric substrates inherently introduce dielectric loss, low-loss materials (like Rogers Duroid 5880, RT/duroid, or other high-performance substrates with low loss tangent) are available. These materials offer low loss tangents (e.g., around 0.0009 for Duroid 5880), which keep dielectric losses to a minimum. By choosing materials with a low loss tangent and by carefully designing the waveguide dimensions, the dielectric loss can be minimized to an acceptable level, allowing for efficient waveguide performance.

In summary, while dielectric substrates in waveguides introduce some dielectric loss, the benefits they provide in terms of compactness, manufacturability, integration, mechanical stability, and cost-effectiveness make them highly valuable, particularly in applications where integration and size constraints are priorities. Advanced low-loss dielectric materials help mitigate the losses, allowing for efficient performance in high-frequency applications where traditional hollow metal waveguides would be impractical.

We have selected **Duroid 5880** as a substrate for Substrate Integrated Waveguide (SIW) structure. Duroid 5880 is a widely used high-frequency laminate from Rogers Corporation, known for its excellent microwave and millimetre-wave performance. It has several properties that make it suitable for SIW applications, including:

Low Dielectric Losses: Low losses help minimize attenuation, which is crucial for long waveguide paths in SIW designs.

Ease of Fabrication: The substrate can be easily processed using standard PCB manufacturing techniques, making it compatible with the via-hole construction required for SIW.

Low Permittivity: A low dielectric constant ($\varepsilon r = 2.2$) results in wider wavelength propagation inside the substrate, allowing for larger SIW dimensions for a given frequency. This is beneficial for fabricating SIW for lower-frequency applications.
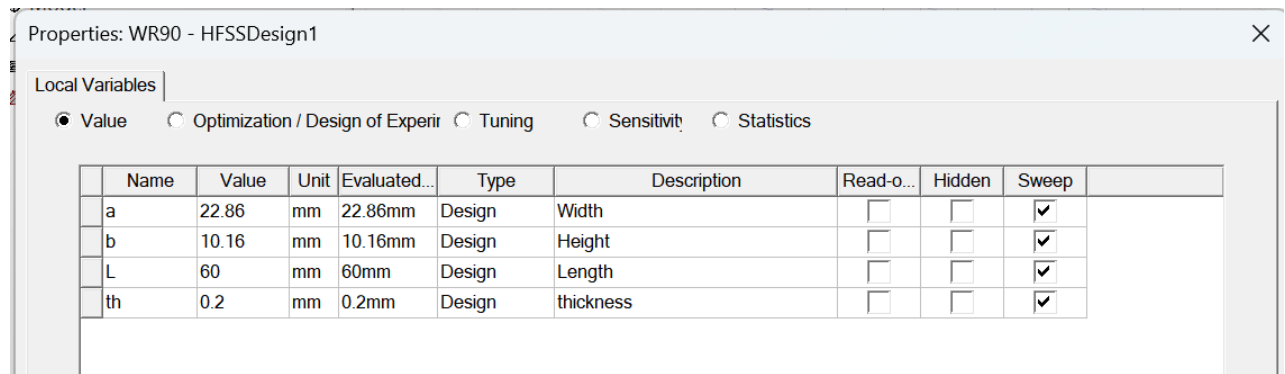
CHAPTER 4: MODELLING THE WAVEGUIDES

For modelling both the waveguides we will be making the use of **ANSYS ELECTRONICS DESKTOP HFSS 2024 R1.** To make minor adjustments in calculations we will also be taking the help of an app called **SIW CAL** which can be downloaded from the app store of your ios device.

4.1 Modelling WR90

We will be taking the recommended specifications for a standard WR90 which has broader dimension (a)= 22.86 mm , and narrow dimension (b)= 10.16mm.

Following are the design properties:

Name	Value	Unit	Evaluated...	Type	Description	Read-o...	Hidden	Sweep
a	22.86	mm	22.86mm	Design	Width	☐	☐	✔
b	10.16	mm	10.16mm	Design	Height	☐	☐	✔
L	60	mm	60mm	Design	Length	☐	☐	✔
th	0.2	mm	0.2mm	Design	thickness	☐	☐	✔

Fig 4.1.1: Local variables chosen in WR90

Here L is the length of the waveguide which does not have any correlation to any propagation characteristics so it can be set to any finite amount. 'th' is the thickness of the copper walls. At 10 GHz (the approximate centre frequency of WR90 operation), the skin depth in copper is roughly 0.66 microns (0.00066 mm**)**. Since the skin depth is so small, any wall thickness much greater than a few skin depths will suffice to contain the fields.

Given below is the hollow metallic box (material assigned is copper):
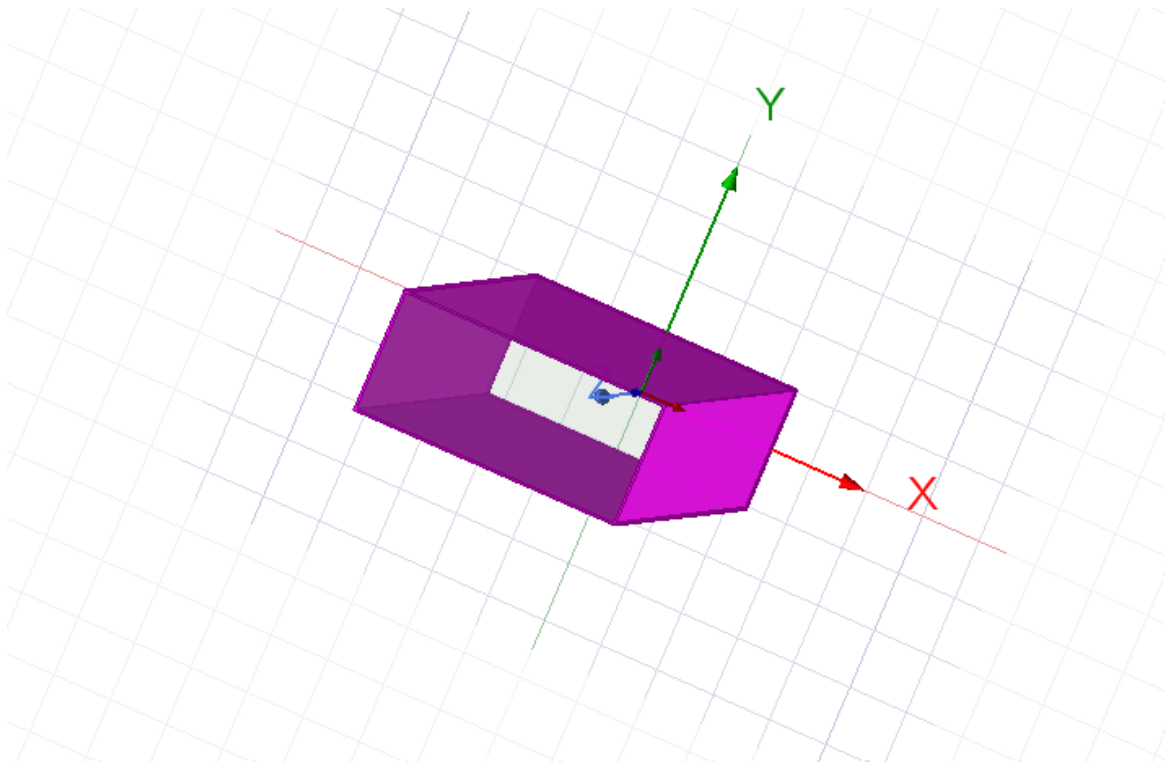
Fig 4.1.2: Hollow metallic structure of WR90

The wave ports assigned at the hollow faces:
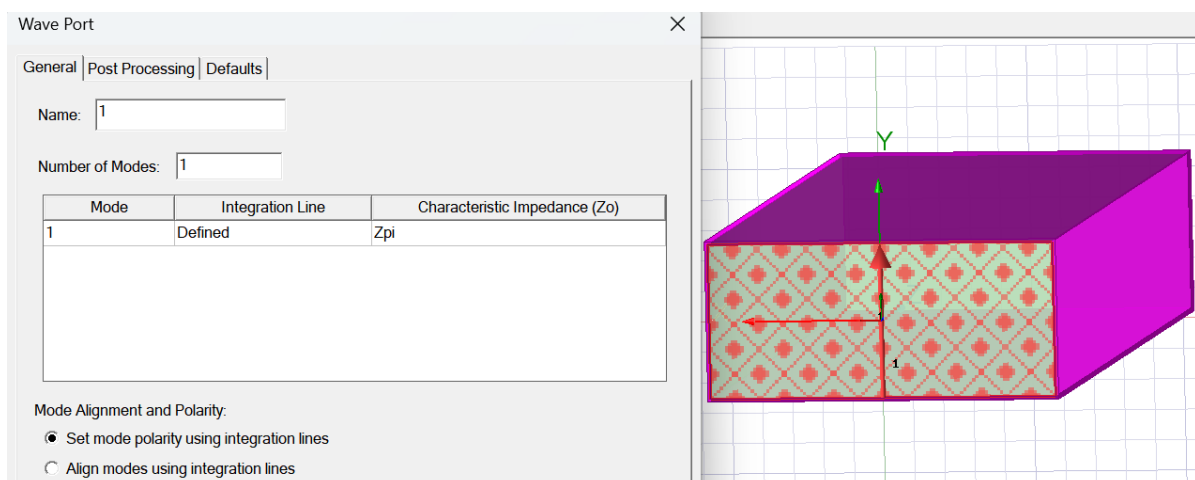
Fig 4.1.3: Assigning Wave port at the hollow face

(Note: The number modes are set to 1 as we will be just observing the characteristics of TE10 mode. For other modes such as TE20, TE01 etc. we can increase the number of modes.)
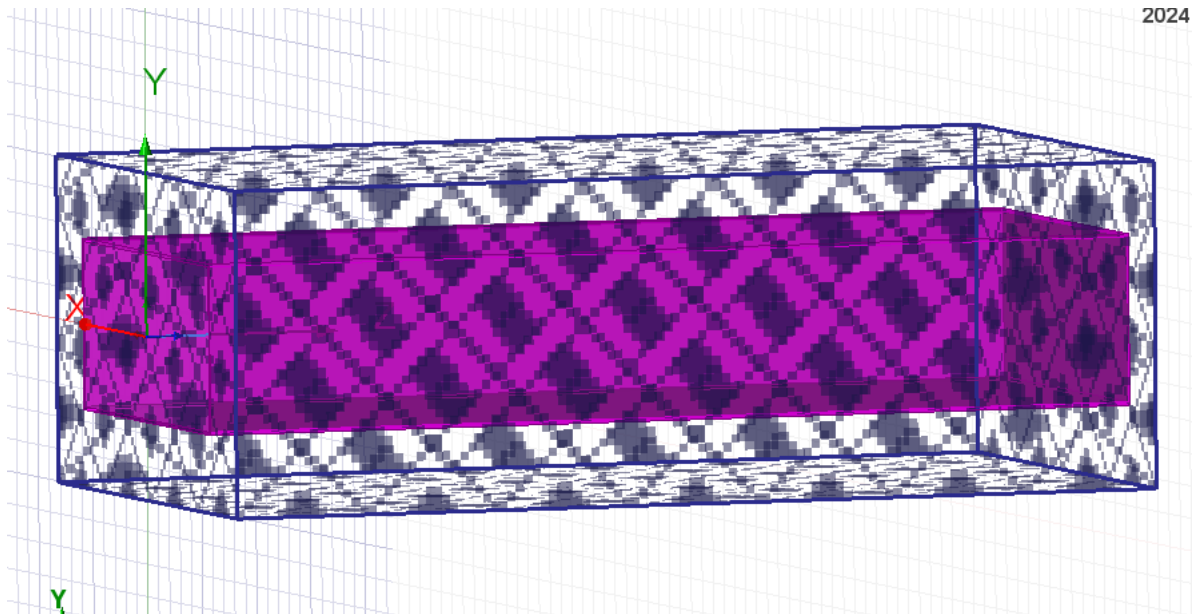
Radiation box encompassing the metal structure:

Fig 4.1.4: Air box with radiation boundary assigned

The physical structure of WR90 is now complete. Now we will move forward towards the analysis and sweep settings.

Fig 4.1.5: Analysis settings of WR90

Here, 10GHz is the operating frequency (recommended EIA standard). We can also increase the number of passes or maximum Delta S for more accurate results.

We will be observing the propagation characteristics of WR90 in range of 5GHz – 17GHz as its recommended working frequency band is from 8.20 to 12.40 GHz.
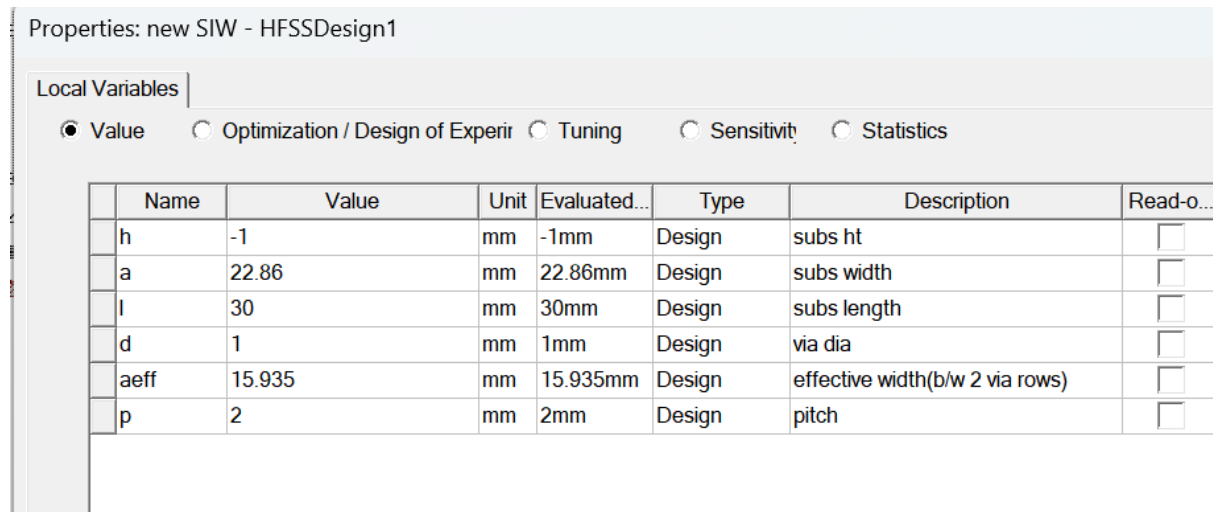
Fig 4.1.6: Sweep settings of WR90

After this, now we Validate and Analyse all the settings but before looking at our results , we will model our custom SIW first and then compare both results side by side.

4.2 Modelling SIW

Following are the design properties of the SIW:

Name	Value	Unit	Evaluated...	Type	Description	Read-o...
h	-1	mm	-1mm	Design	subs ht	☐
a	22.86	mm	22.86mm	Design	subs width	☐
l	30	mm	30mm	Design	subs length	☐
d	1	mm	1mm	Design	via dia	☐
aeff	15.935	mm	15.935mm	Design	effective width(b/w 2 via rows)	☐
p	2	mm	2mm	Design	pitch	☐

Fig 4.2.1: Local variables chosen in SIW

Here substrate height 'h' is taken to be 1mm. Substrate thickness (h) Typical values range from **0.254 mm** to **1.524 mm** depending on the application. For high-frequency applications, thinner substrates (e.g., 0.254 mm or 0.508 mm) are often used. 'a' is the physical width of the substrate which is taken same as in WR90. 'l' is the physical length which is also taken the same as in WR90 case.

'd' is taken to be 1mm. The via diameter 'd' is typically chosen to be **1/5 to 1/10** of the guided wavelength λg at the operating frequency (which is 10GHz in this case).

Pitch 'p' is generally twice the via diameter so its taken as 2mm.

'aeff' is the distance between the two rows of vias. It is taken to be 15.935mm and is calculated by equations discussed in previous sections.
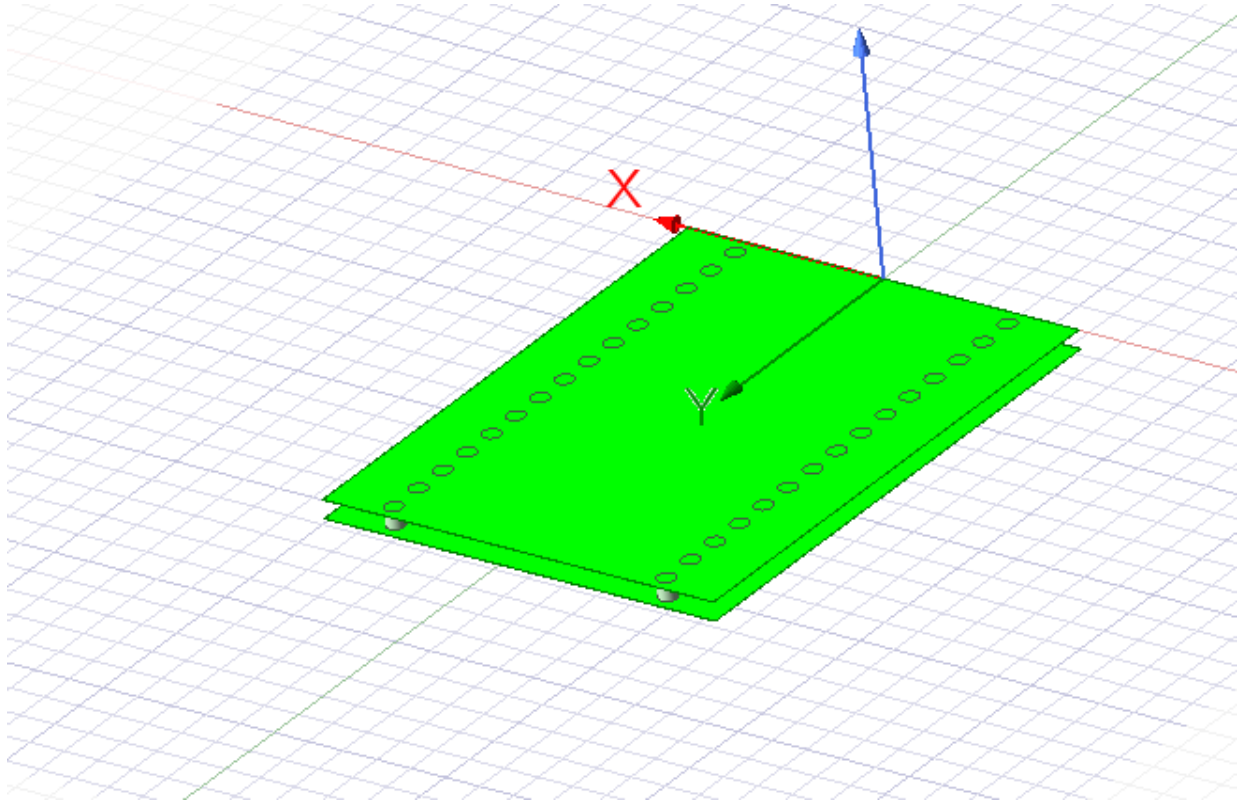
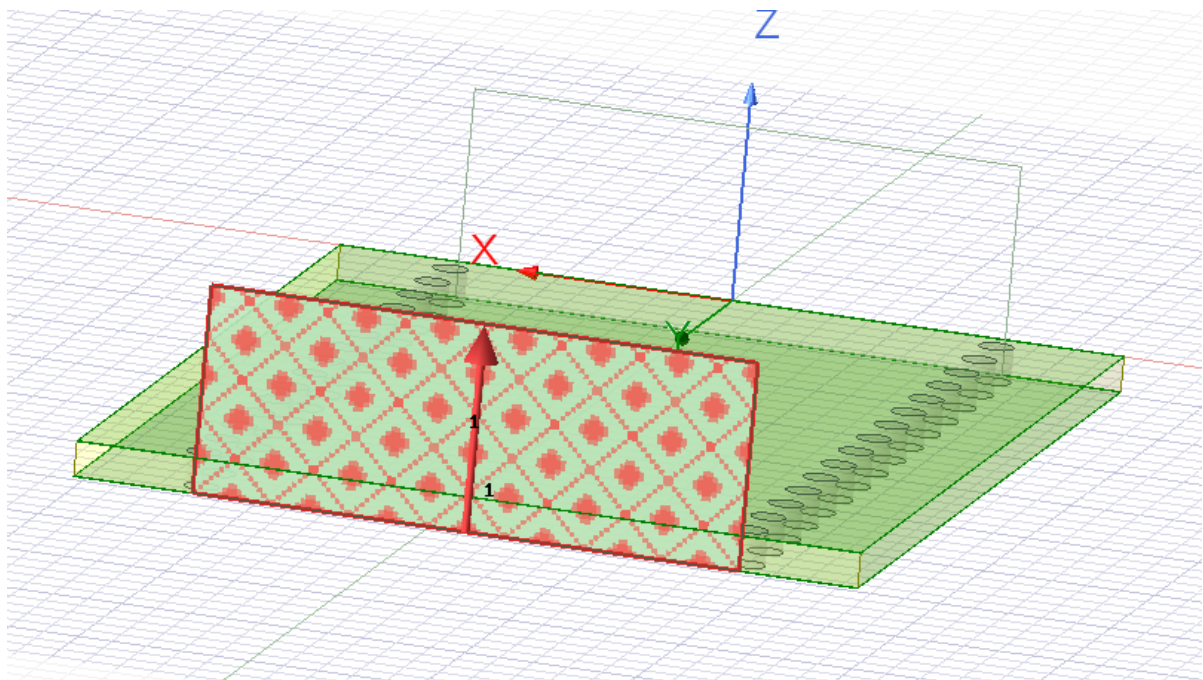**Fig 4.2.2: Design of Substrate Integrated Waveguide (SIW) in HFSS**
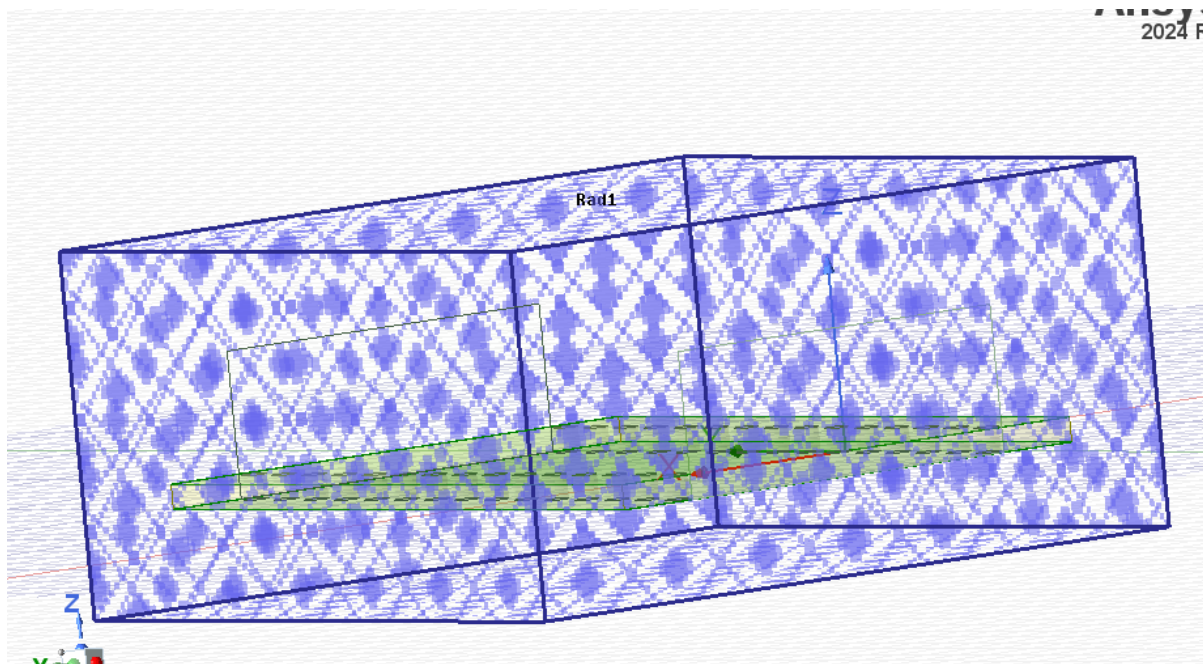

Fig 4.2.3: Wave port excitation in SIW

Fig 4.2.4: Radiation Box encompassing SIW

Fig 4.2.5: Advanced analysis settings

Fig 4.2.6: Sweep frequency range

CHAPTER 5: RESULTS AND COMPARISONS

In this section we are going to analyse and compare both the waveguides on parameters such as S- Parameters, wave propagation in TE10 mode, losses experienced, phase constant, and electric field distributions. All the results are simulated at 10GHz operating frequency.
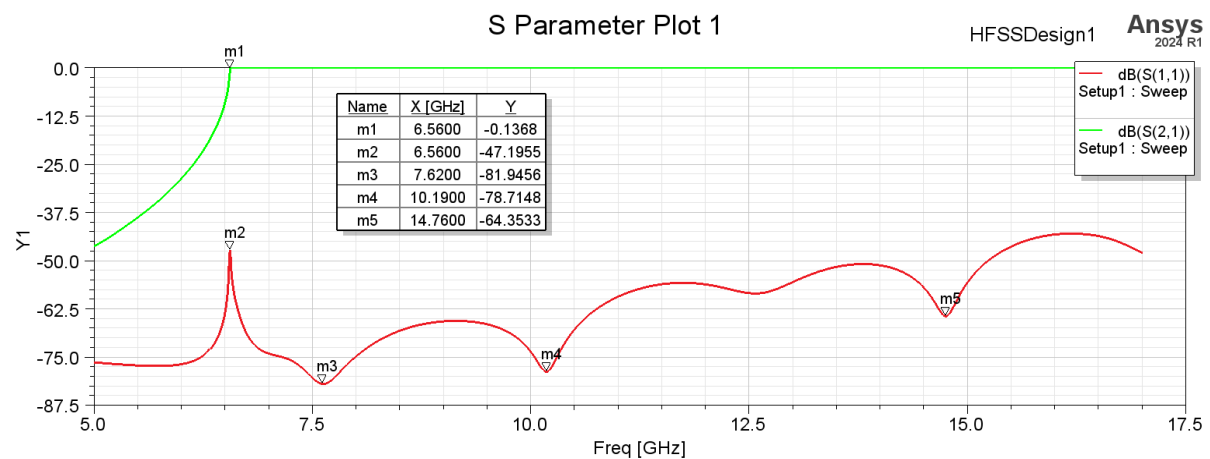
5.1 Plots

    (1)   S-Parameters

Fig 5.1.1: S-Parameter plot of WR90

For the above plot, the S21 (insertion loss) parameter (green curve) begins to rise around 6.56 GHz, which aligns with the expected cutoff frequency of WR90 for the dominant TE10 mode (approximately 6.56 GHz). This indicates that the WR90 waveguide begins supporting propagation around this frequency. The plot is relatively smooth, indicating **lower insertion loss** across the frequency range, which is expected for a metallic waveguide with minimal dielectric losses

The S11 (return loss) parameter (red curve) shows a corresponding peak around 6.56 GHz, suggesting a reflection peak at the cutoff point, which is typical as fields start to propagate.
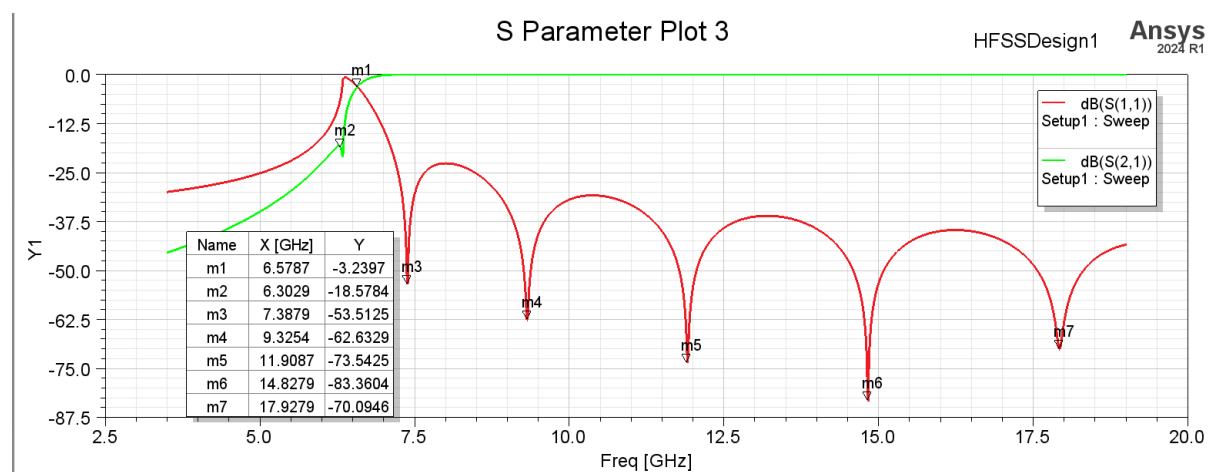

Fig 5.1.2: S-Parameter plot of SIW

The SIW also shows a rise in S21 at approximately 6.57 GHz. This close match with the WR90 cutoff frequency suggests that the SIW design effectively matches the WR90 waveguide cutoff. The S21 transmission characteristic is less stable for the SIW. There are noticeable peaks and dips at frequencies like 7.39 GHz, 9.32 GHz, and beyond. These dips in S21 suggest leakage that could be affecting the SIW. The fluctuating response for the SIW suggests that it might have **higher insertion losses**, likely due to **dielectric losses** in the substrate

The S11 for the SIW also peaks around this frequency, similar to the WR90, indicating the onset of propagation.

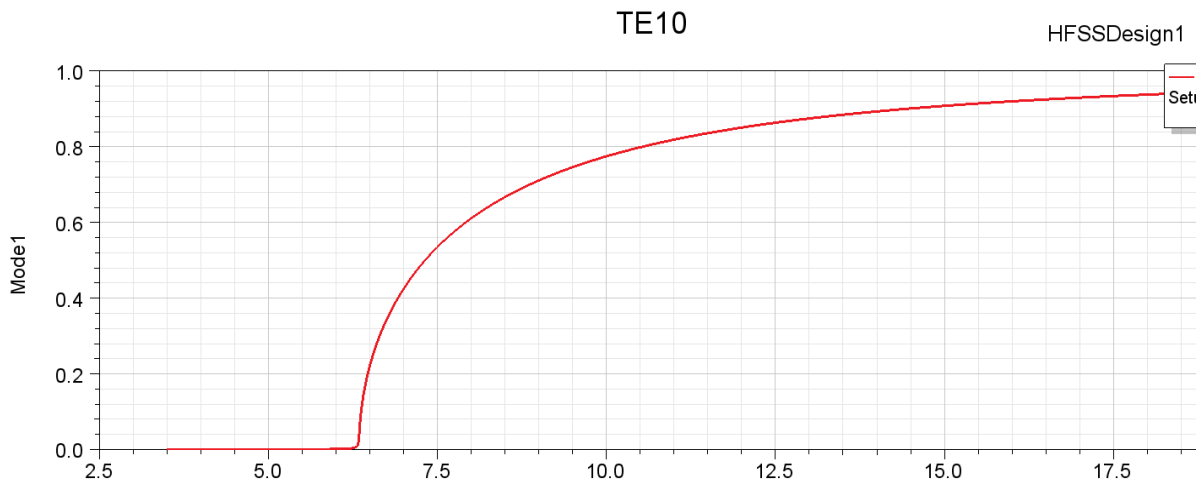**(2) TE10 Mode Propagation**

Fig 5.1.3: Propagation in TE10 mode (SIW)

For SIW, TE10 grows more rapidly above the cutoff, indicating higher attenuation per unit length. This is due to the combined effects of dielectric, leakage, and conduction losses in the SIW. The steeper slope in SIW suggests that losses become more pronounced at higher frequencies, potentially due to increased dielectric loss and leakage.

While SIW provides better integration and compactness, its higher attenuation at and above cutoff highlights its lossy nature, especially at higher frequencies. This may limit its application where low-loss performance is critical. The attenuation can be mitigated with design optimizations such as reducing via pitch and diameter or using lower-loss dielectric materials.
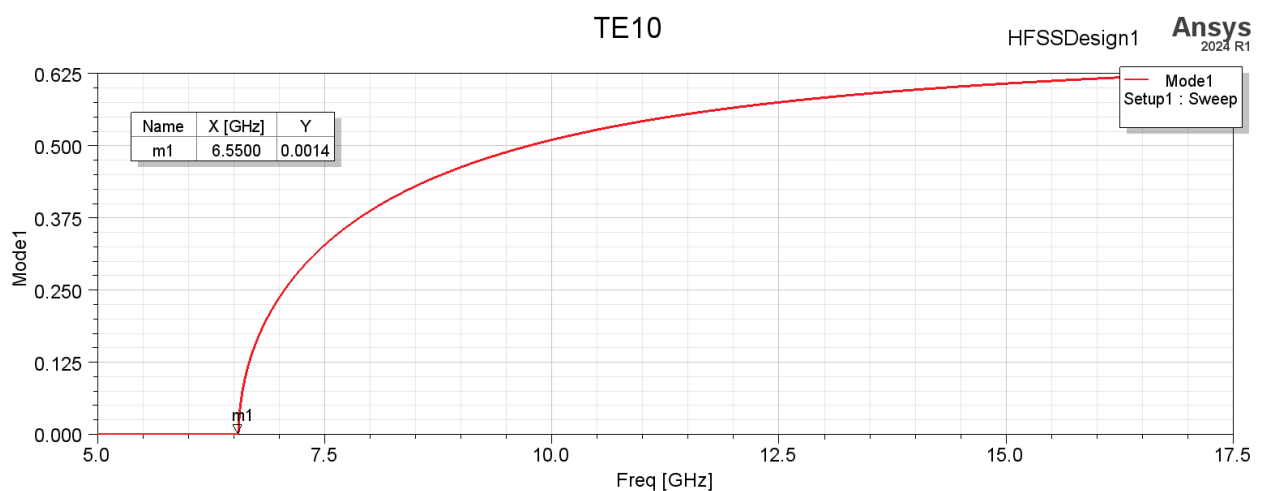

Fig 5.1.4: Propagation in TE10 mode (WR90)

For WR90, Mode1 increases more gradually, reflecting lower overall losses, as WR90 experiences negligible dielectric loss and no leakage. WR90's shallower slope indicates that it maintains better efficiency over a broader frequency range. WR90 exhibits superior performance in terms of attenuation characteristics, making it a better choice for applications

23

where efficiency and low loss are essential. Its consistent attenuation across the frequency range ensures better phase stability and power transmission.
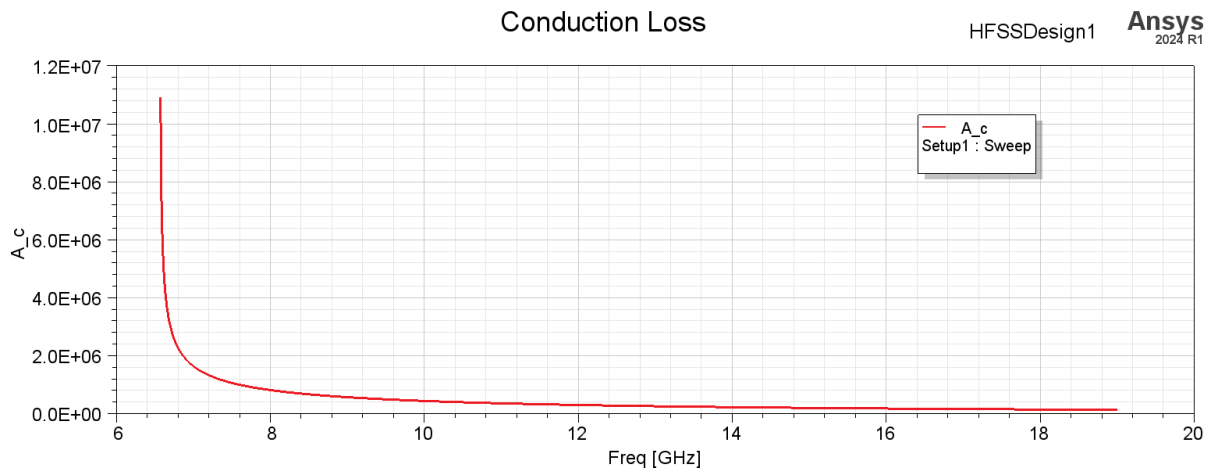
(3)   Conduction Loss

Fig 5.1.5: Conduction loss in SIW

The conduction loss for the SIW shows a **rapid decline as frequency increases**. It starts at a relatively high value around 10 MHz at 6 GHz and drops to nearly zero around 13 GHz and above. This trend suggests that conduction loss in the SIW is initially significant at lower frequencies but becomes minimal at higher frequencies.
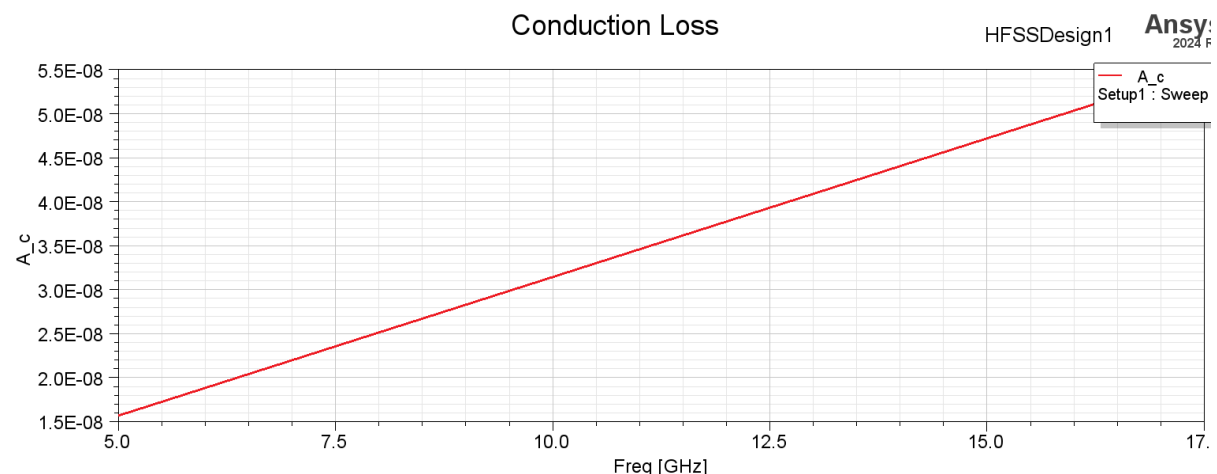

Fig 5.1.6: Conduction loss in SIW

The WR90 waveguide behaves as expected, with conduction losses that linearly increase with frequency due to the increased surface resistance. This is typical for an air-filled metallic waveguide, where conduction loss dominates.

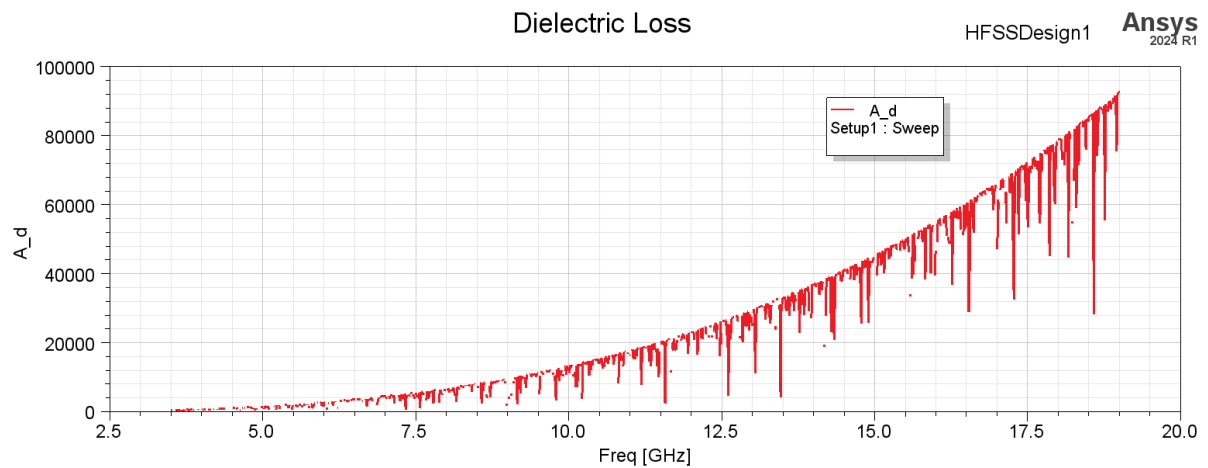**(4) Dielectric Loss**

Fig 5.1.7: Dielectric loss in SIW

The dielectric loss in the SIW increases with frequency, as seen in the dielectric loss plot. This trend is consistent with the use of a dielectric substrate (e.g., Duroid 5880), where the loss tangent causes increased dielectric loss at higher frequencies. However, the plot also has sharp dips or fluctuations at certain frequencies, which could be due to resonances or numerical artifacts. Interpolating with many frequency points (e.g., 1201) over a wide range can occasionally produce these numerical artifacts.
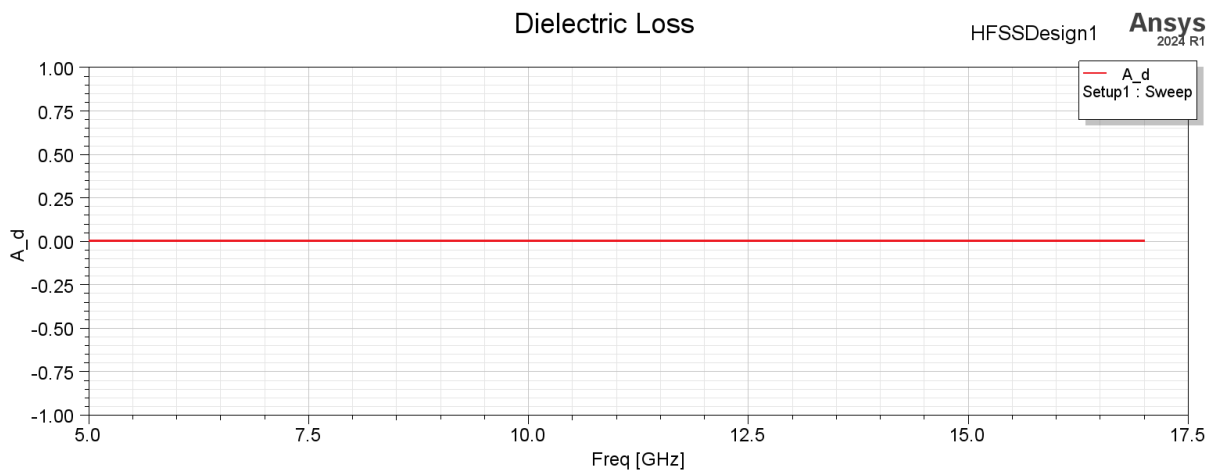

Fig 5.1.8: Dielectric loss in WR90

Since WR90 is typically air-filled, the dielectric loss is negligible or zero in our case.
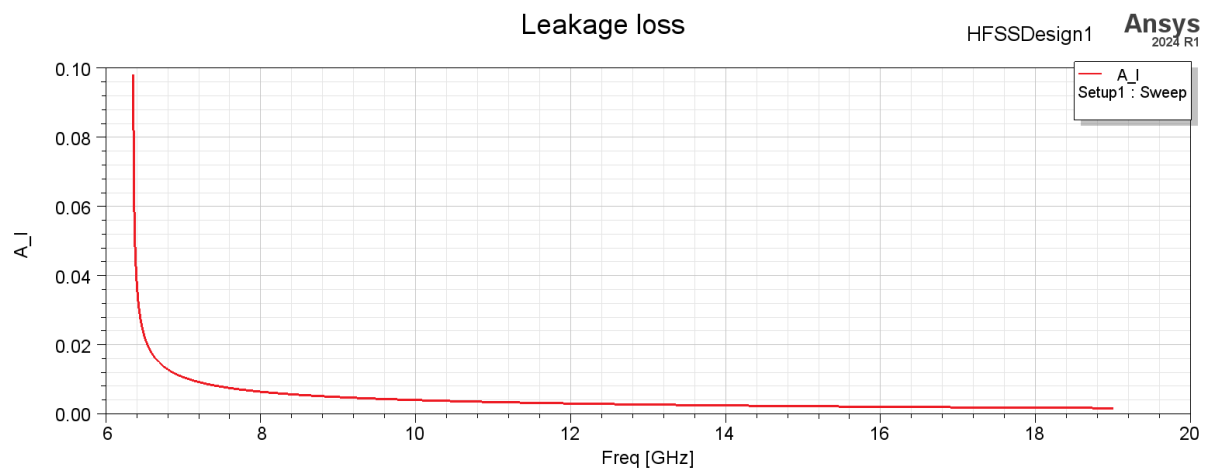
(5)   Leakage loss

Fig 5.1.9: Leakage loss in SIW

Leakage loss is exclusive to SIWs only because of existence of vias. As the frequency increases, the leakage loss sharply declines and approaches near-zero values above approximately 12 GHz. At higher frequencies, the quasi-TE10 mode becomes better confined within the SIW structure, and the periodic vias act as more effective sidewalls, reducing the amount of field energy that can leak out. This improvement in confinement at higher frequencies results in significantly lower leakage loss, allowing the SIW to perform more similarly to a traditional waveguide.
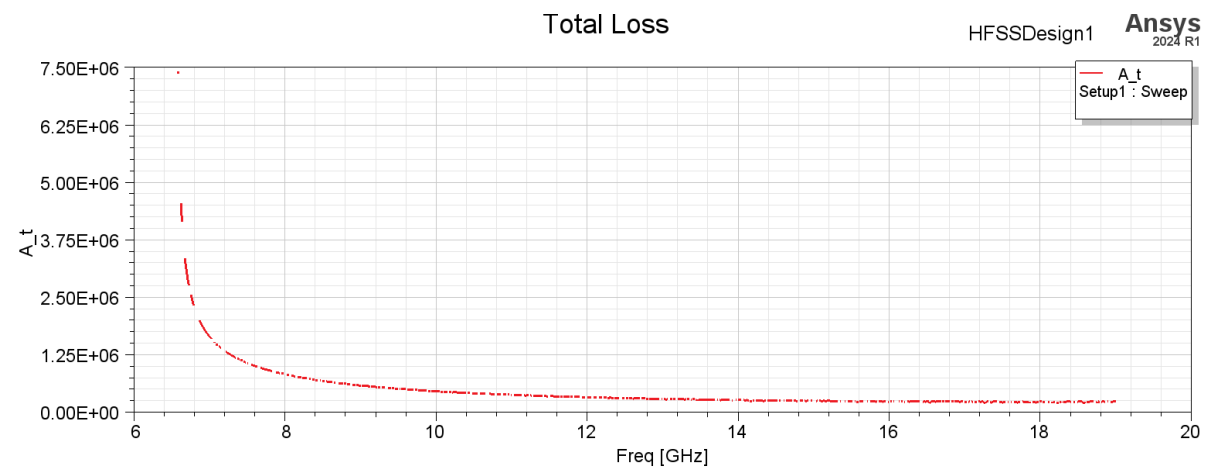
(6)   Total loss

Fig 5.1.10: Total loss in SIW

The total loss in the SIW is high at lower frequencies (around 6 GHz) and then quickly declines as frequency increases, stabilizing to a lower loss level above approximately 10 GHz. The trend aligns with typical SIW behaviour, where lower frequencies show higher losses due to less effective mode confinement and leakage, while higher frequencies stabilize as dielectric loss becomes the primary contributor.

Fig 5.1.11: Total loss in WR90

The WR90 shows a **linear increase in total loss** as frequency increases, which is expected due to the conduction loss in the metallic walls.

Since WR90 is an air-filled waveguide with no significant dielectric, **dielectric loss remains constant at zero** (as confirmed in previous data). Thus, the total loss in WR90 is almost entirely due to **conduction loss** on the metallic walls, which increases with frequency because of the decreasing skin depth.

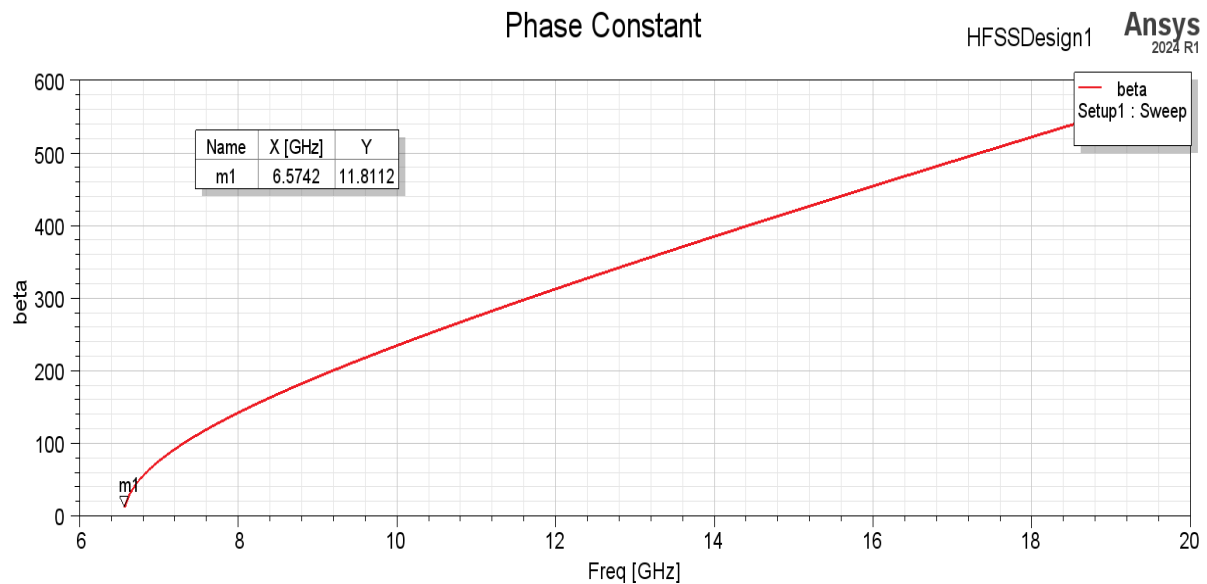### (7)   Phase Constant (Beta)

Fig 5.1.12: Phase constant in SIW

Similar to WR90, the phase constant starts near zero at the cutoff frequency (~6.57 GHz) and rises with frequency. However, the phase constant for SIW increases more steeply, especially at higher frequencies, indicating that the propagation characteristics in SIW are more strongly influenced by the dielectric substrate, which increases the effective permittivity and slows down the wave propagation, leading to a higher phase constant for a given frequency.
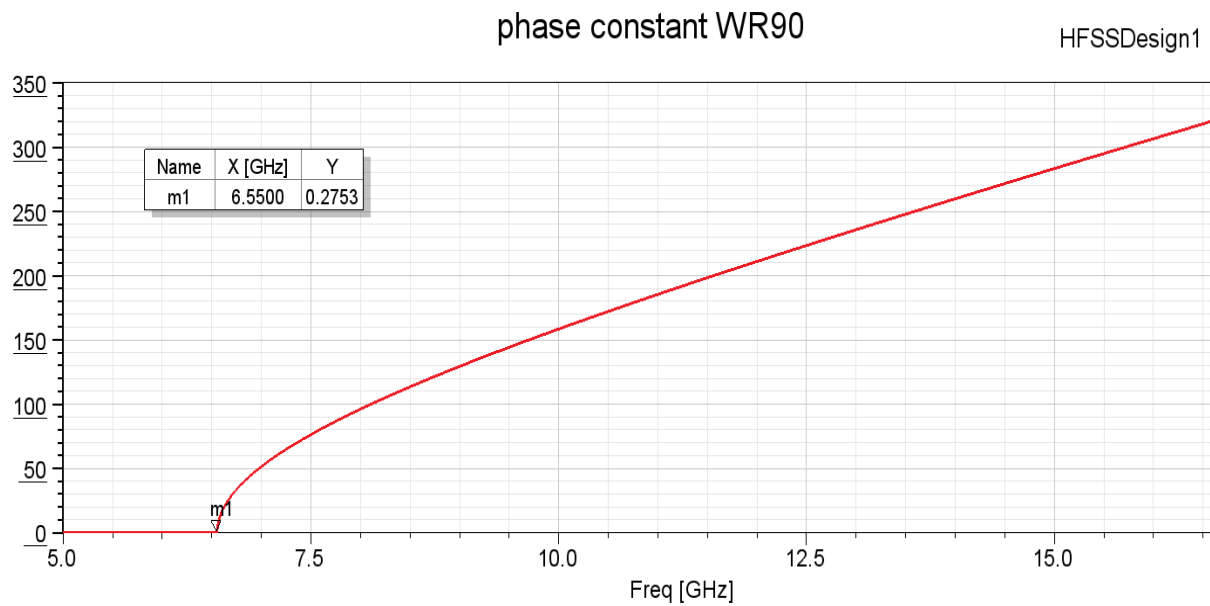
phase constant WR90

Name	X [GHz]	Y
m1	6.5500	0.2753

Fig 5.1.13: Phase constant in WR90

The phase constant starts from zero at the cutoff frequency (~6.55 GHz) and increases approximately linearly as the frequency increases. This behaviour is expected for a waveguide operating in its dominant mode (TE10), where the propagation becomes more efficient above the cutoff frequency. The phase constant is lower due to the air-filled structure, allowing for faster propagation of waves with less dispersion. WR90 is ideal for applications requiring minimal phase distortion and consistent propagation characteristics, such as high-frequency radar systems or satellite communication.

5.2 Output variables

Following are the output variables assumed which were integral in plotting the above results. The theory behind these variables is referenced in [2][7].

Output Variables

☑ Validate output variables for selected context

	Name	Expression
1	A_c	Rs*((2*10.16*3.142*3.142) + (22.86^3)*k0^2)/ ((22.86^3)*10.16*k0*n)
2	A_d	(k0^2)*0.0009/2*beta
3	A_t	A_c + A_d
4	Mode1	im(Gamma(1))/k0
5	Rs	sqrt(2*pi*u/(2*5.8*10^7))
6	beta	sqrt(k0^2 - kc^2)
7	e	2.2*8.854*10 ^(-12)
8	fc	6.56*10^9
9	k0	2*3.142*freq*sqrt(u*e)
10	kc	2*3.142*fc*sqrt(u*e)
11	n	sqrt(u/e)
12	u	4*pi*10^(-7)

Fig 5.2.1: Output variables in WR90

	Name	Expression
1	A_c	Rs / (Te *n * sqrt(1 - (fc^2 / freq^2))) * (Te + (2 * fc^2 / freq^2))
2	A_d	(k0^2)*0.0009/2*kz
3	A_l	((1 / aeff) * (d / aeff)^2.84 * ((p / d) - 1)^6.28) / (4.85 * ((2 * aeff / Lamba_d)^2 - 1)^0.5)
4	A_t	A_c + A_l +A_d
5	Lamba_d	(3e8)/(freq*sqrt(2.2))
6	Mode1	im(Gamma(1))/k0
7	Rs	sqrt(2*pi*freq*u/2*5.8*10^7)
8	Te	aeff- (d^2/(0.95*p))
9	beta	sqrt(k0^2 - kc^2)
10	e	2.2*8.854*10 ^(-12)
11	fc	(3e8)/(2*Te*sqrt(2.2))
12	j	im(1)
13	k0	2*3.142*freq*sqrt(u*e)
14	kc	2*3.142*fc*sqrt(u*e)
15	kz	sqrt(k0^2 -((2/Te)* tan((fc/freq)*Rs*(1-i)))^2)

Fig 5.2.2: Output variables in SIW
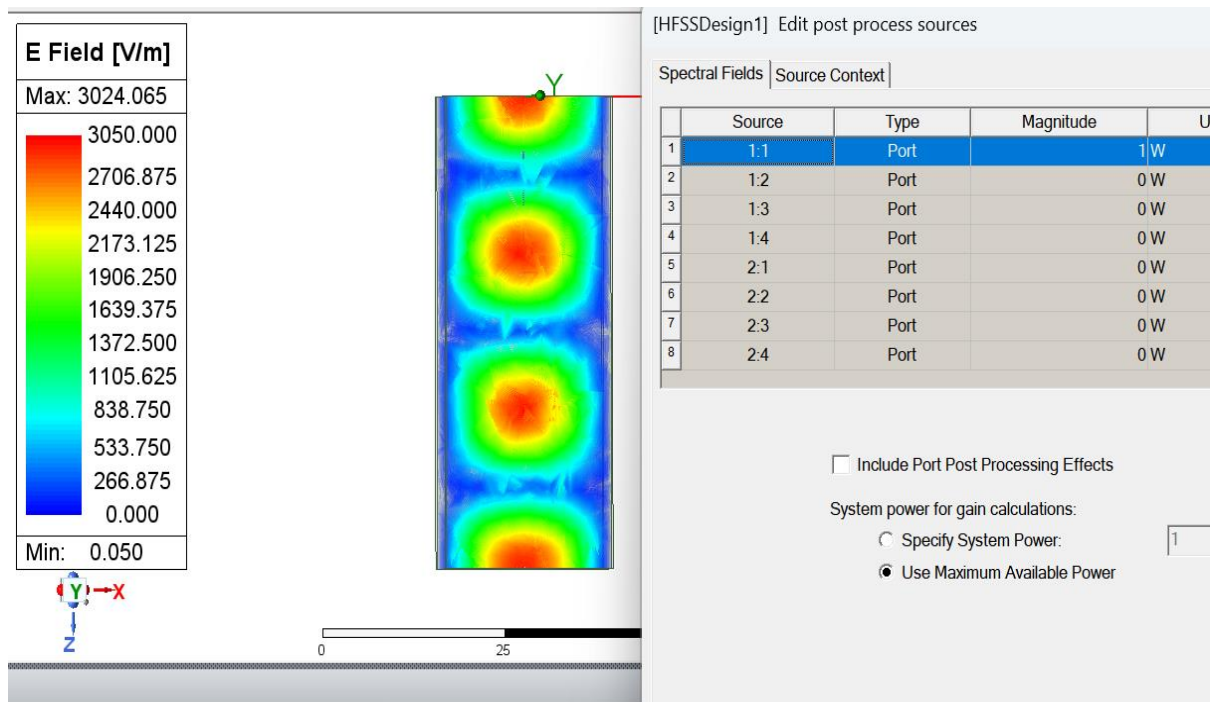
5.3 Electric Field Distribution

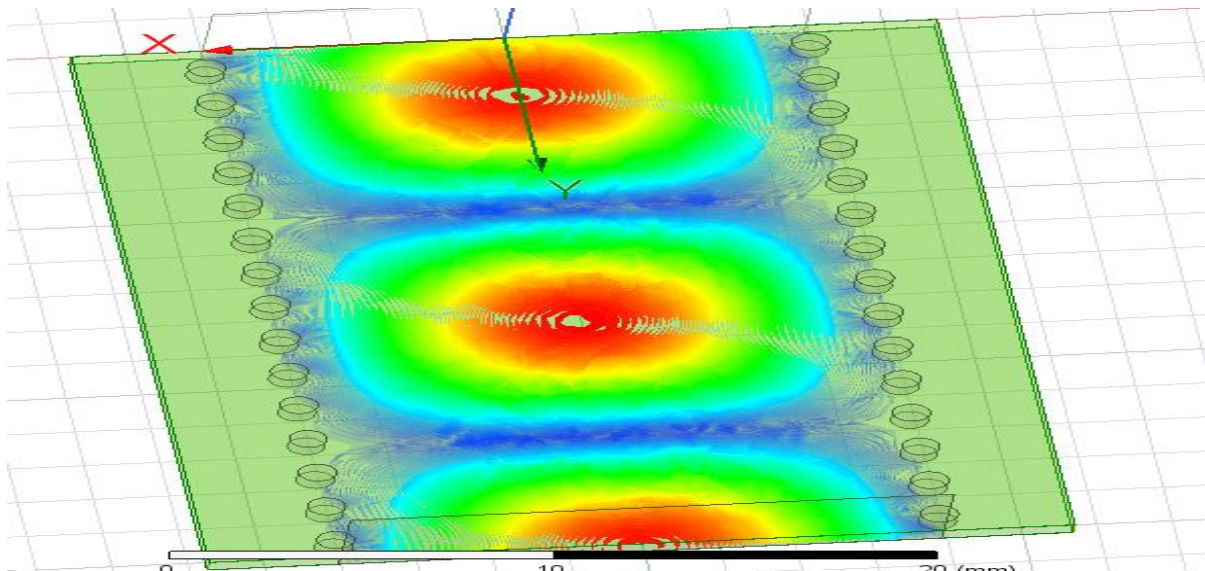**Fig 5.3.1: Magnitude of E-Field pattern in WR90 (TE10)**

Fig 5.3.2: Magnitude of E-Field pattern in SIW (TE10)

The E-field patterns in both WR90 and SIW show a periodic distribution of field peaks along the length of the waveguide, which aligns with the quasi-TE10 mode typically supported by SIWs. This mode structure resembles the field distribution seen in a traditional rectangular waveguide. Each red-coloured peak in the E-field magnitude represents an area of maximum

electric field intensity, while the blue regions indicate areas of minimal field strength (nodes), showing the typical standing wave pattern within the waveguide.

The WR90 waveguide's E-field pattern demonstrates efficient propagation of the TE10 mode with strong field confinement and minimal losses. This efficiency makes WR90 ideal for applications where low-loss, high-power transmission is required, such as radar systems, satellite communications, and other high-frequency applications. However, its bulkiness and lack of planar integration make it less suitable for compact systems compared to SIW.

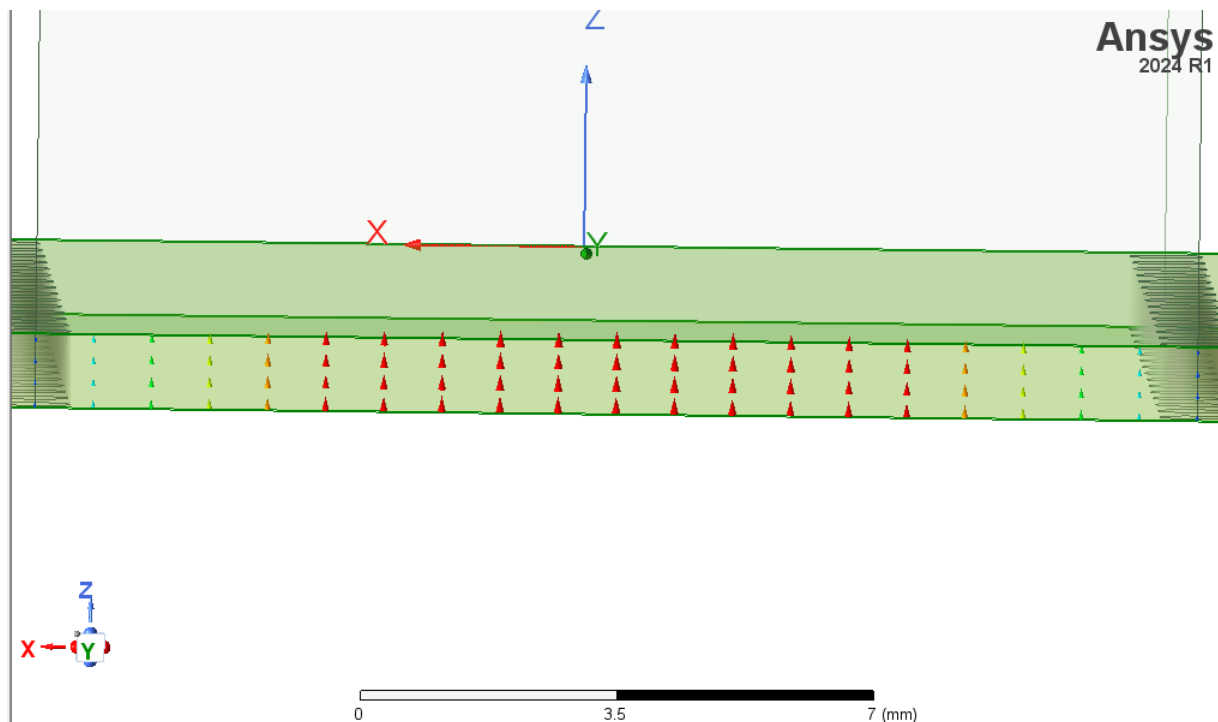Following are the fields present at the wave port:

Fig 5.3.3: Port Field Display in SIW (TE10)

The field pattern in the SIW is also close to a quasi-TE10 mode, with a strong electric field in the central region. However, there may be slight asymmetry or distortion near the edges where the via rows confine the fields. The arrows indicating field strength are fairly uniform across the width, but due to the presence of the dielectric substrate and the periodic vias, there may be slight fringe effects or non-uniformities, especially at higher frequencies.

This quasi-TE mode behaviour in the SIW mimics the WR90's TE10 mode, confirming that the SIW design effectively supports similar field characteristics within the guiding region.
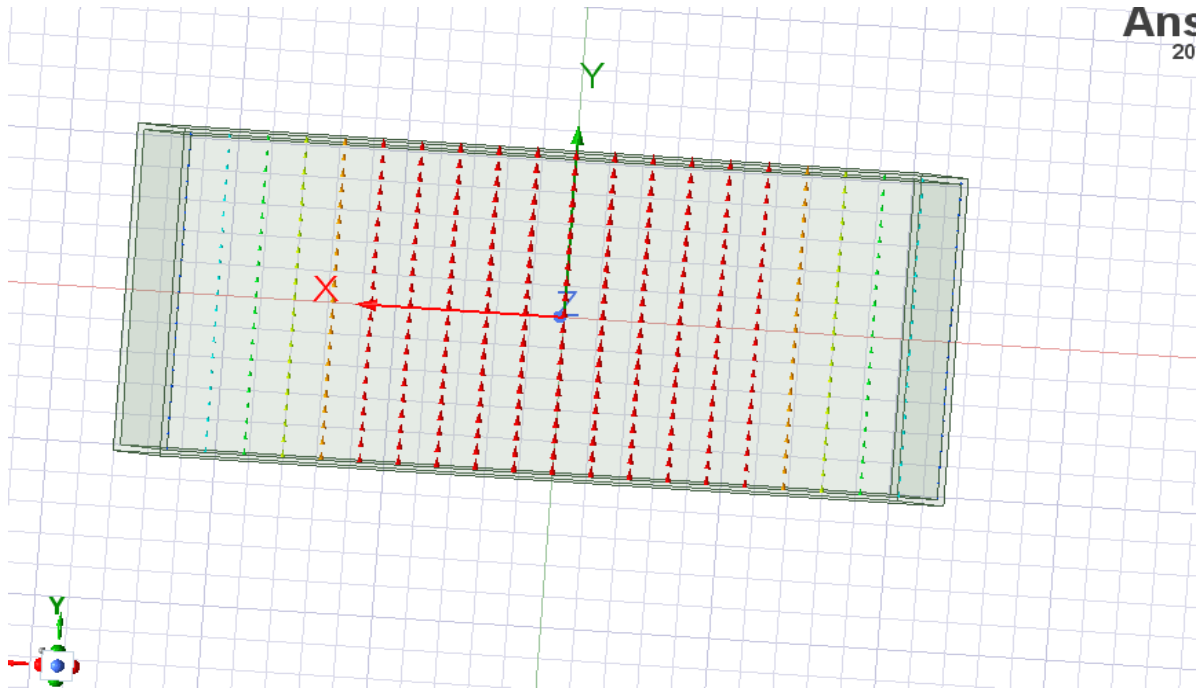
Fig 5.3.4: Port Field Display in WR90 (TE10)

The field distribution shows a clear TE10 mode, which is characterized by a single peak in the electric field across the width of the waveguide. The red arrows indicate that the electric field is strongest at the centre, tapering off towards the sides, which aligns with the expected field pattern for the TE10 mode in a rectangular waveguide. This mode indicates efficient wave propagation with minimal interference or distortion, as would be expected in an ideal metallic waveguide with no dielectric losses.
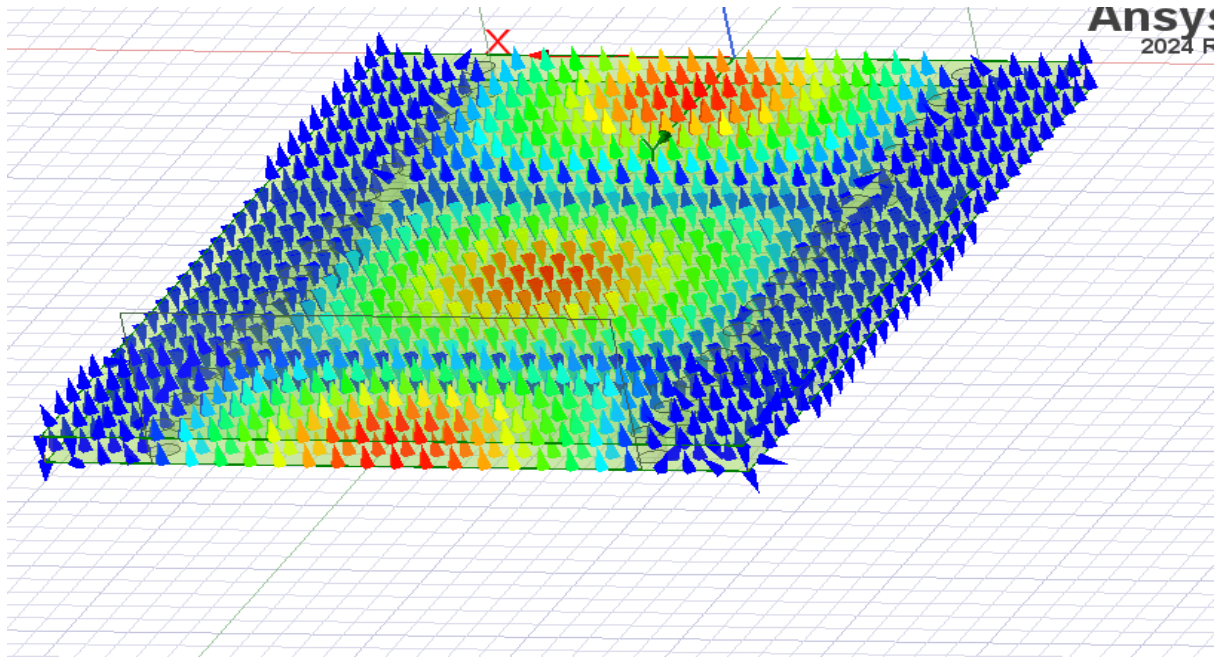
Fig 5.3.5: Vector E-Field pattern in SIW

The E-field vectors in the SIW structure show a similar quasi-TE10 pattern to the WR90, with areas of high field strength near the centre and lower field intensity near the edges. However, due to the presence of the dielectric substrate and the rows of vias, the pattern is slightly modified compared to the WR90. The vias partially confine the fields, but there are some fringing effects and minor variations in the field direction near the via regions. These fringing effects are expected in SIWs due to the nature of the partial confinement, as opposed to the solid metallic walls in WR90.
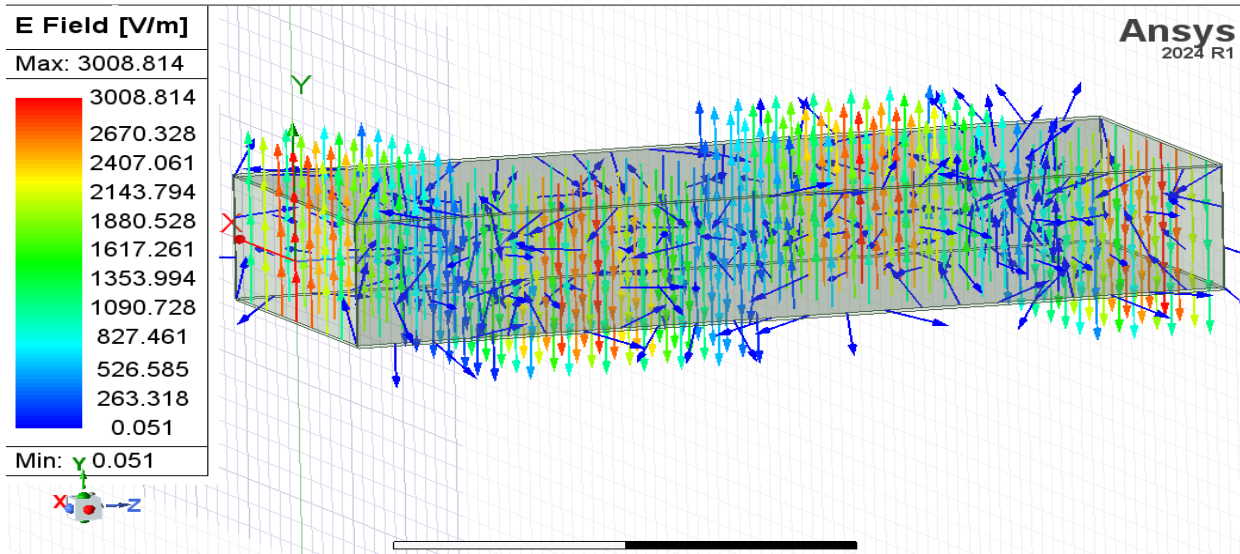
Fig 5.3.6: Vector E-Field pattern in WR90

The E-field vectors show a clear, well-defined pattern characteristic of the TE10 mode. In this mode, the electric field is strongest at the centre of the waveguide and weakens toward the walls, with the field vectors oriented perpendicular to the waveguide's propagation direction. Since WR90 is a metallic waveguide with air as the medium, the fields are tightly confined within the waveguide walls. This confinement ensures minimal interaction with the outside, which is why the WR90 is **highly efficient with lower overall losses.**

CHAPTER 6: CONCLUSION

Most of the characteristics of our SIW designed and WR90 are similar. The major point of difference comes when comparing the losses experienced by both the waveguides. This study compares the performance characteristics of a Substrate Integrated Waveguide (SIW) and a WR90 rectangular waveguide by analysing key parameters such as S-parameters, electric field distribution, and total losses across a range of frequencies.

Both the SIW and WR90 support a TE10 mode or its equivalent, with a similar central peak in the electric field across the waveguide width. The SIW supports a quasi-TE mode, which closely resembles the TE10 mode in WR90 but with minor variations due to its dielectric substrate and partial confinement by rows of metallic vias. The WR90 exhibits a more symmetrical and confined field pattern, whereas the SIW experiences slight fringing and leakage due to the via-based confinement. The WR90 shows lower total loss overall, with losses primarily due to conduction on the metallic walls. Since it is air-filled, dielectric loss is negligible, resulting in high efficiency across its operating bandwidth. The SIW has a more complex loss profile due to the combination of dielectric, conduction, and leakage losses. At lower frequencies, conduction and leakage losses are more prominent, while at higher frequencies, dielectric loss in the substrate (Rogers 5880) becomes the dominant factor. This leads to higher total loss in the SIW, particularly at lower frequencies, making it less efficient than WR90. Both waveguides exhibit similar cutoff frequencies for the TE10 mode, but the SIW's cutoff is slightly shifted due to the dielectric substrate and periodic vias. At higher frequencies, **WR90 outperforms SIW in efficiency** due to its negligible dielectric losses and lower total loss. For applications operating in the upper frequency range, WR90 would be the preferred choice for minimizing signal attenuation, while SIW may be better suited for applications where compact design and integration with planar circuits are more critical than maximum efficiency.

WR90 is highly efficient, with low losses across its frequency range, making it ideal for applications that require minimal loss and tight field confinement. Meanwhile, SIW exhibiting higher loss, offers advantages in size reduction and integration with planar circuits, making it suitable for compact and integrated microwave systems where some additional loss is acceptable. The SIW provides a compact, integrable solution that approximates the TE10 mode structure. The trade-offs between size and efficiency should be considered based on application needs: WR90 for high-efficiency, low-loss applications and SIW for compact, planar systems with moderate loss tolerance.

This conclusion is neither meant to debunk all the other works done on the subject of SIW nor it is claiming that there is no reason to use SIWs over any air-filled waveguides. If SIWs are constructed with better optimisation techniques, they can outperform their rectangular waveguide counterparts (with same dielectric substrate) provided that the leakage losses in SIW are kept to minimum, as found out in conclusion of [7]. In scenarios where space, integration, and cost are primary concerns, such as 5G antennas, phased array systems, and compact RF modules, SIW's planar design and compatibility with PCB processes make it a

better choice than WR90. While WR90 offers lower loss in standalone, high-efficiency applications, it lacks the form factor and integration ease needed for many modern compact RF systems. SIW can be fabricated using standard PCB manufacturing processes, allowing it to be seamlessly integrated with other RF, microwave, or digital components on the same substrate. This is a significant advantage in complex systems where the waveguide needs to connect directly with microstrip lines, coplanar waveguides, or other planar circuit elements.

The purpose of this report was just to provides a comprehensive comparison of the SIW and WR90 waveguides, summarizing their respective strengths and limitations, and guides the choice of waveguide structure based on specific application requirements.

<u>REFERENCES</u>

1. D. Sharma, S. Kumar, and S. Kumar, "Design and Simulation of Substrate Integrated Waveguide and Substrate Integrated Waveguide Antennas," *IOSR Journal of Electronics and Communication Engineering (IOSR-JECE)*, vol. 15, no. 2, pp. 18-24, Mar.-Apr. 2020. DOI: 10.9790/2834-1502011824.

2. D. Deslandes and K. Wu, "Accurate Modeling, Wave Mechanisms, and Design Considerations of a Substrate Integrated Waveguide," *IEEE Transactions on Microwave Theory and Techniques*, vol. 54, no. 6, pp. 2516-2526, June 2006. DOI: 10.1109/TMTT.2006.875807.

3. R. Bochra, M. Feham, and J. Tao, "Analysis of S-Band Substrate Integrated Waveguide Power Divider, Circulator and Coupler," STIC Laboratory, University of Tlemcen, Tlemcen, Algeria, and LAPLACE Laboratory, INP-ENSEEIHT Toulouse, University of Toulouse, Toulouse, France.

4. A. O. Nwajana and E. R. Obi, "A Review on SIW and Its Applications to Microwave Components," Electronics, vol.11, no.7, p.1160, Apr.2022. DOI: 10.3390/electronics11071160.

5. A. Banwari, S. Gotra, Z. Hashim, and S. Saxena, "Design of Chamfered H-bend in Rectangular Substrate Integrated Waveguide for K-band Applications,"Journal of Microwave and Optical Technology.

6. H. Kumar, R. Jadhav, and S. Ranade, "A Review on Substrate Integrated Waveguide and its Microstrip Interconnect,"Journal of Electronics and Communication.

7. "Propagation Characteristics of SIW and Waveguide: A Comparison," in *Nanoelectronics, Circuits and Communication Systems*, S. Kumari, V. R. Gupta, and S. Srivastava, Eds. Springer, Jan. 2021. DOI: 10.1007/978-981-15-7486-3_50.